JOURNAL OF MATERIALS SCIENCE **34** (1999) 1025–1030

TEM observation of DO_3 structure in Fe_3Al alloy with Mn addition

B. Y. LOU
Department of Mechanical Engineering, Zhejiang University of Technology, Hangzhou, 310014, P. R. China

X. ZHANG, M. LIU, Z. MAO
Department of Material Science and Engineering, Zhejiang University, Hangzhou, 310027, P. R. China

The structures of DO_3 Fe-28Al-1.5Mn alloy, including ordering degree, superdislocation, APD and APB, were investigated by TEM. The results showed that addition of manganese into DO_3 Fe_3Al could not change the ordered type of the alloy, but could reduce APD size and then reduce ordering degree of the alloy. The fourfold superdislocations were retarded in DO_3 Fe_3Al alloy after Mn addition. Undeformed alloy with Mn has mainly twofold superdislocations. As deformation increases, the twofold superdislocations slip and decompose into unit dislocations, and unit dislocations slip and slip cross, leading to better ductility. The deformation mechanism of DO_3 Fe-28Al-1.5Mn alloy was controlled at first by twofold superdislocation and at last by unit superdislocation. © *1999 Kluwer Academic Publishers*

1. Introduction

In recently years there are more and more studies on iron aluminides such as DO_3-ordered Fe_3Al alloys because of their low cost, high oxidation and sulfidation resistance, and relatively high strength at elevated temperature. In particular, DO_3 Fe_3Al alloys are very attractive for structure applications at medium temperature in many industries because of their positive temperature dependence of strength. However, like other ordered alloys, their poor ductility at room temperature is an obstacle to their engineering application. Some studies have shown that the lack of ductility in DO_3 Fe_3Al alloys is related to their superlittic structure. Carwfold *et al.* [1] observed superdislocations in DO_3 Fe_3Al-based alloy by weak-bundle transmission microscopy and found fourfold superdislocations existing in the alloy. Other researchers confirmed that fourfold superdislocation has lower energy than twofold superdislocation and unit dislocation, and then is more stable in DO_3 Fe-28Al alloy [2, 3]. It is known that the existence of fourfold superdislocation is the major reason for the difficult deformation of DO_3 Fe_3Al alloy. Mckamey *et al.* [4] investigated APBs in DO_3 Fe-28Al alloy and found that APB energies, E_{NNAPB} and E_{NNNAPB}, are high (where NNAPB and NNNAPB represent nearest-neighbor and next-nearest-neighbor antiphase boundaries respectively), reaching up to 79 and 64 (erg/cm^2) respectively, R_1 and R are only 7 and $25 \sim 37$ nm respectively, and slip lines are few and linear in the deformed alloy, showing difficult slip and cross slip of the superdislocations and little active slip systems when the alloy deformed. Research by Morris *et al.* has further shown [5] that the deformation behavior of the alloy is controlled by different mechanisms according to ordering degree in the alloy. Deformation behavior is controlled by unit-dislocation motion when the ordering degree is low, but controlled by superdislocation motion if the alloy is in high order condition. Some other studies have shown that fine grains and addition of ternary elements could reduce APB energy or change APB type, which propagate slips and cross slips in the alloy. For example, TiB_2 could reduce grain size and APB energy in Fe-28Al ordered alloy, especially greatly reducing E_{NNNAPB} to 46 (erg/cm^2), promoting motion of superdislocation [4]. Cr is an effective element to improve the ductility of DO_3 Fe_3Al alloy. Cr addition could reduce E_{NNAPB} and E_{NNNAPB} to $29 \sim 35$ and 28 (erg/cm^2) respectively and then superdislocations could more easily decompose, slip and slip cross in the alloy when the alloy deformed, leading to good ductility [4–6]. Recently, some attention has been paid to Mn, and it has been found that Mn addition could improve mechanical properties of DO_3 Fe_3Al and B_2 FeAl alloys [7,8], but it is not known about the mechanism for Mn influence on properties of the alloys. Our preliminary studies have shown that Mn is an effective element for improving room temperature ductility and strength of DO_3 Fe-28Al alloy [9, 10]. The present paper tries to focus our attention on the microstructure of the alloy with Mn addition. In this work, the ordering degree, superdislocation, antiphase domain (APD) and antiphase domain boundary (APB) of DO_3 Fe-28Al-1.5Mn alloy are investigated by transmission electron microscopy (TEM). The alloys are chosen and examined before deformation, after deformation and after fracture, respectively.

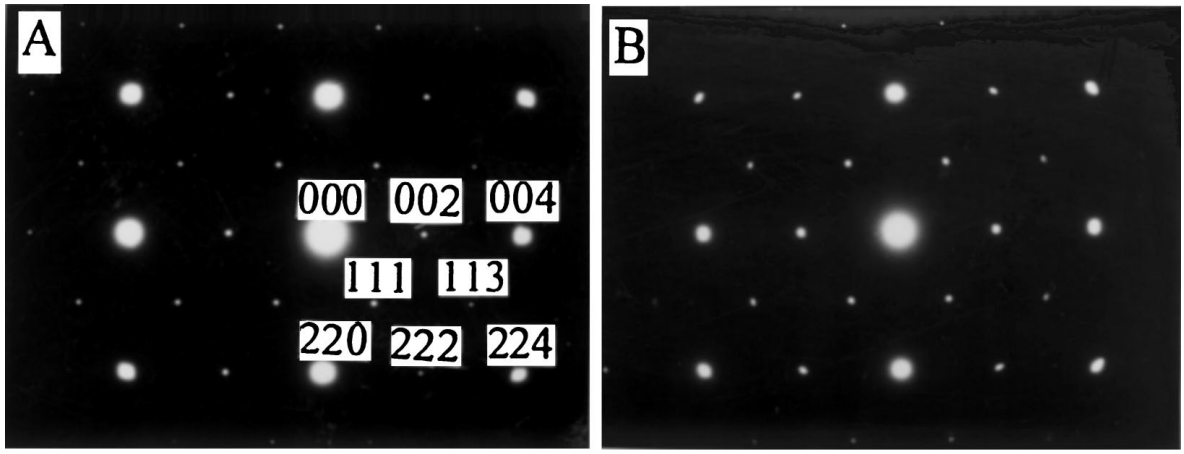

Figure 1 Electron diffraction patterns of Fe-28Al-1.5Mn alloy (a) and Fe-28Al alloy (b) in [$\bar{1}$ 1 0].

2. Experimental procedures

The DO_3 Fe_3Al intermetallics studied were Fe-28% Al and Fe-28% Al-1.5% Mn (atomic percent) alloys. Both alloys were smelted in a vacuum induction furnace and cast into iron molds. After homogenizing for 4 h at 950 °C, the alloys were hot-rolled at 950 °C and warm-rolled at 650 °C from 7 mm to 0.7 mm.

Tensile samples with a gauge section of $0.7 \times 5 \times 20$ mm were punched from the rolled sheet, and then heat treated in air for 1 h at 800 °C (for recrystallization) plus 50 h at 450 °C (for DO_3 ordering).

Thin foil samples were prepared from undeformed and deformed tensile samples to examine the state of order, antiphase domain (APD) and antiphase boundary (APB). These thin foil samples were prepared by spark cutting 3 mm disks from the 0.7 mm thick samples, gliding to 0.1 mm, and electropolishing in a fresh solution of one part nitric acid to four parts methanol in a Tenupol twin jet system at about −5 °C and 8 V. TEM examination was carried out using a Philips CM12 electron microscope operating at 120 kV.

X-ray diffraction samples for ordering study were cut from the sheets by spark machining, with gauge dimension of 10 mm width, 14 mm length, and 0.7 mm thickness, following mild abrasion to remove the oxide coating. X-ray diffractometer traces were obtained from these samples using a Rigaku D/MAX-3BX operated at 50 kV, 25 mA, producing Mo-Kα radiation. Measurements were performed by step scanning 2θ from 10° to 90° with a 0.3° step size. A count time of 1 min. per step was used.

3. Experimental results

3.1. Ordering state

In DO_3 structure, the fundamental reflections occur for $h+l+k=2n$ (where n is an integer) and DO_3 reflection occurs where h, l and k are odd [11]. The observation of the diffraction pattern shows that the Fe-28Al-1.5Mn alloy has DO_3 ordering structure after 50 h ordering treatment at 450 °C. Mn addition could not change the order type in that alloy. Fig. 1 shows superlattices of the alloys with and without Mn addition in [$\bar{1}$10] diffraction pattern. As Fig. 1 shows, strong fundamental spots are (0 0 4), (2 2 0) and (2 2 4), and weak superlattice spots are (1 1 1) and (1 1 3). The degree of DO_3 ordering was determined by the following relation [12]:

$$S = K\sqrt{\frac{I_{(1\,1\,1)}}{I_{(2\,2\,0)}}} \tag{1}$$

where $I_{(1\,1\,1)}$ is integral strength of 1 1 1 superlattice diffraction, $I_{(2\,2\,0)}$ is integral strength of 2 2 0 fundamental diffraction, and K is a constant related to $I_{(1\,1\,1)}$ and $I_{(2\,2\,0)}$. Compared with Fig. 1a and 1b, it can be seen that the relative strength of superlattice diffraction spots to fundamental diffraction spots in Fe-28Al alloy is stronger than that in Fe-28Al-1.5Mn alloy, suggesting that Mn could weaken superlattice diffraction of DO_3 Fe_3Al and decrease the degree of DO_3 ordering.

TABLE I XRD measurements on (1 1 1) and (2 2 0) planes

Alloy	2θ	I	hkl	$I/I_{(2\,2\,0)}$
Fe-28Al	12.220	262	111	3
	19.900	10252	220	100
Fe-28Al-1.5Mn	12.220	403	111	2
	19.960	23581	220	100

In order to illustrate further the effect of Mn on ordering in the alloy, both alloys are analyzed by XRD. The results of superlattice diffraction strength $I_{(1\,1\,1)}$ and fundamental strength $I_{(2\,2\,0)}$ by XRD are shown in Table I. It is obvious from Table I that the alloy without Mn addition has higher ratio $I_{(1\,1\,1)}$ to $I_{(2\,2\,0)}$ than the alloy with Mn addition, demonstrating further that Mn decreases the ordering degree.

3.2. Dislocation configuration

In general, there exist fourfold superdislocations in undeformed DO_3 Fe-28Al alloy [1–3]. After Mn was added into the alloy, no fourfold superdislocations could be observed in all orientation of foil. There exist twofold dislocations in undeformed DO_3 Fe-28Al-1.5Mn alloy. Fig. 2 shows the superdislocation configuration in $\mathbf{g}=220$ under $+\mathbf{g}/-\mathbf{g}$ condition. As Fig. 2 shows, there are two types of Burgers vector, $\mathbf{b}_1$ and $\mathbf{b}_2$.

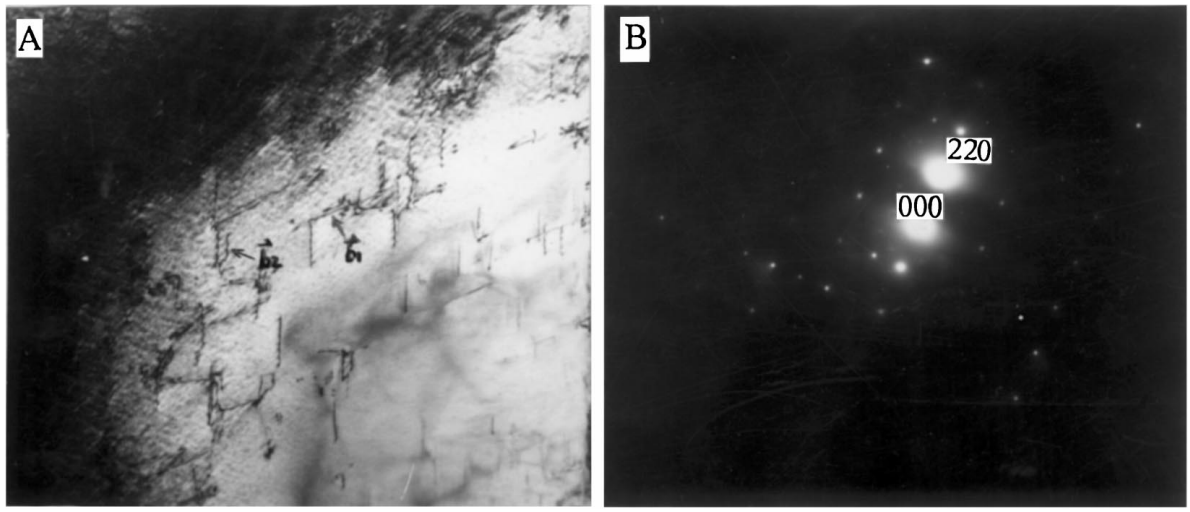

Figure 2 (a) Bright-field micrograph of superdislocations obtained under $+\mathbf{g}/-\mathbf{g}$ condition, (b) selected diffraction pattern obtained within area of micrograph shown in Fig. 2(a).

TABLE II Determination of Burgers vector

		g		
b		220	112	$\bar{2}02$
$\mathbf{b}_1$	$11\bar{1}$	Visible	Not visible	Visible
$\mathbf{b}_2$	$1\bar{1}1$	Visible	Visible	Not visible

The dislocations with $\mathbf{b}_1$ could not be visible in $\mathbf{g} = 224$ and could be visible in $\mathbf{g} = \bar{2}02$. On the other hand, the dislocations with $\mathbf{b}_2$ could be visible in $\mathbf{g} = 224$ and could not be visible in $\mathbf{g} = \bar{2}02$. According to the unseen rule of dislocation $\mathbf{g} \cdot \mathbf{b} = 0$, it is found that $\mathbf{b}_1$ and $\mathbf{b}_2$ are [1 1 1] and [1 1 1] respectively, as shown in Table II, and then slip plane and direction calculated are {1 1 0} and ⟨1 1 1⟩ respectively, suggesting that Mn addition could not change slip systems in the alloy.

Fig. 3 shows the change in superdislocation configuration when the alloy deformed. Twofold superdislocation moved and decomposed gradually into unit dislocations and unit dislocations slipped and slipped cross during deformation (Fig. 3b). As the deformation continued, the amount of unit dislocations increased, and more slip and cross slip led to twine in the dislocations. There are completely twined dislocations in the fractured alloy (Fig. 3d). Measured by the weak-beam method, the space, R of twofold superdislocation as shown in Fig. 3a is about $50 \sim 100$ nm, which is larger than that in DO_3 Fe-28Al alloy [4].

3.3. APD and APB configuration

In general, ordering is a diffusive procedure. During ordering, the order domain forms, grows and at last the alloy consists of many antiphase domains (APDs). The DO_3 Fe_3Al alloy typically has two types of APD: thermal APD and deformed APD. Fig. 4 shows APD at $\mathbf{g} = 1\,1\,1$. It can be seen from Fig. 4a that APBs are isotropic and smooth. APD size is about $150 \sim 250$ nm, which is smaller than that in the alloy without Mn addition. The APD size of $250 \sim 400$ nm is reported for DO_3 Fe_3Al alloys without ternary elements [13, 14]. During deformation, the configuration of APBs is gradually changed from random curves into crossed lines and deformed APBs. Fig. 4b shows some deformed APBs occuring after the alloy deforms slightly ($\varepsilon = 0.3\%$). Thermal APBs are changed into deformed APBs completely in the sample of $\varepsilon = 1.5\%$ (Fig. 4c) and the density of deformed APBs increases (Fig. 4c and 4d). It is indicated from Fig. 4 that the APBs increase as deformation increases, suggesting that superdislocations induce more deformed APBs in the specimen during gliding. There was a large number of zigzag APBs in the fractured sample, as shown in Fig. 4d. The existence of zigzag APBs also suggests that cross slips of dislocation took place frequently when the alloy deformed. To examine further the increase in slip and cross slip of the alloy after Mn addition, deformed samples (1.5% plastic strain) were prepared under tension at room temperature. Slip lines on the surfaces of both alloys are shown in Fig. 5. In Fig. 5a, straight slip lines are parallel to each other and aligned in the same direction within individual grains on the surface of the Fe-28Al alloy, suggesting that little cross slipping happens and only one slip system is generated in this alloy. In contrast, slip lines in the Fe-28Al-1.5Mn alloy become finer, denser and apparently wavy (Fig. 5b), and some slip lines even pass through grain boundaries, indicating that not only slip is more likely to take place but cross slip is also generated during deformation in the alloy after Mn addition.

4. Discussion

The TEM observation results have shown that manganese addition has reduced the ordering degree and APD size, retarded formation of fourfold dislocation, and increased twofold superdislocation's separation, decomposition and motion. Those are related to change in the ordering energy of the alloy after Mn addition.

Mn atoms are soluble in the DO_3 Fe_3Al alloy. The line scanning of Mn K_α of DO_3 Fe-28Al-1.5Mn alloy in Fig. 6 shows that the distribution of manganese is even

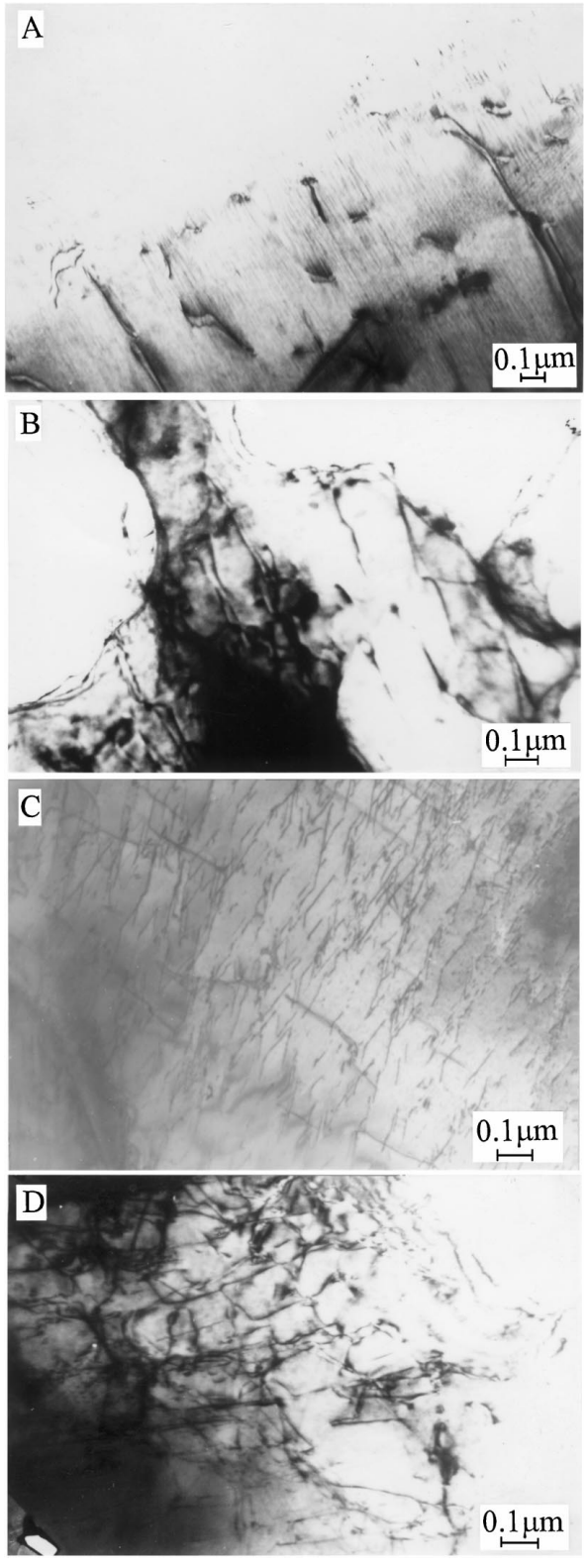

Figure 3 Bright-field micrographs of superdislocation configuration in DO_3 Fe-28Al-1.5Mn alloy deformed in different amount of plastic deformation. (a) $\varepsilon = 0.3\%$, (b) $\varepsilon = 1.0\%$, (c) $\varepsilon = 2.0\%$, (d) fracture.

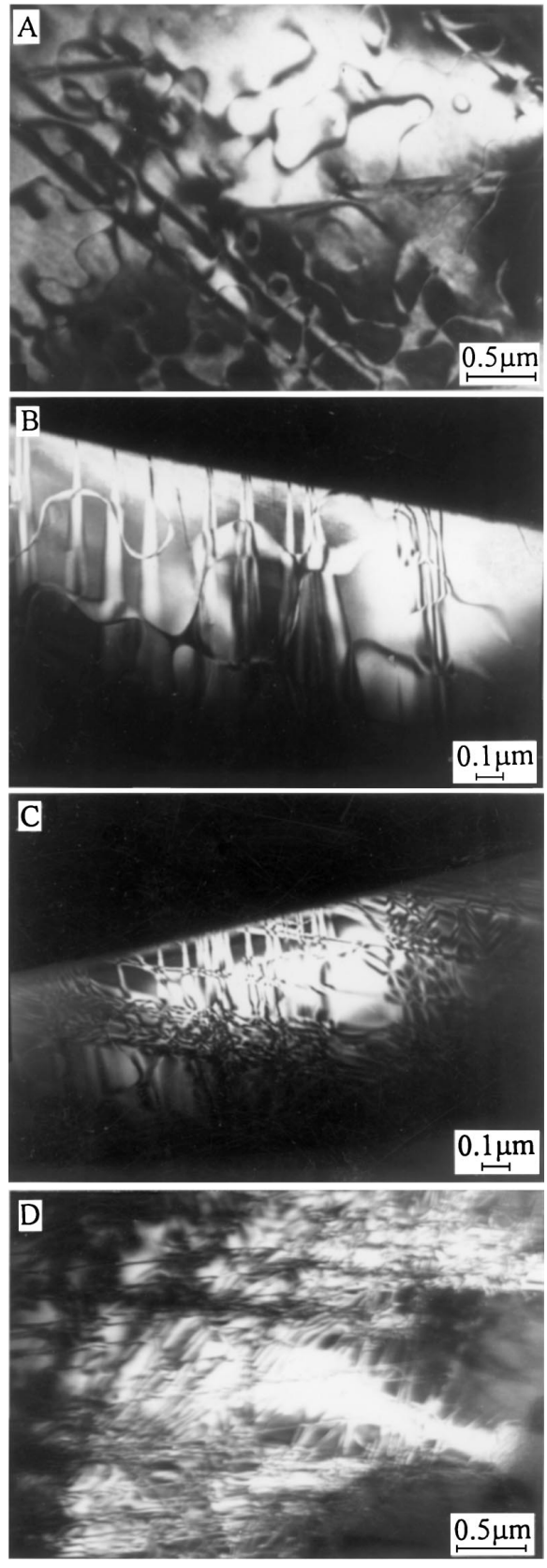

Figure 4 Bright-field micrograph of APD_s and APB_s obtain in $\mathbf{g} = 1\,1\,1$ under $+\mathbf{g}/-\mathbf{g}$ condition. (a) underformed, (b) $\varepsilon = 0.3\%$, (c) $\varepsilon = 1.5\%$, (d) fracture.

in the alloy and no significant enriching of manganese is found at grain boundaries or in the grains, indicating that solubility limit of Mn in the alloy has not been reached. The solubilized Mn could change the ordering energy of the alloy. The DO_3 Fe-28Al alloy is rich in Al atoms and lacking in Fe atoms and further more, Mn-Al ordering energy is much lower than Fe-Mn ordering energy [15]. So Mn atoms will occupy Fe atom sites after Mn addition into the alloy. Among Fe, Al and Mn elements, the electronegativities of Fe, Al and Mn are 1.8, 1.5 and 1.5 respectively. The electronegative difference between Al and Mn is zero, less than that between Al and Fe atoms or Mn and Fe atoms, leading to

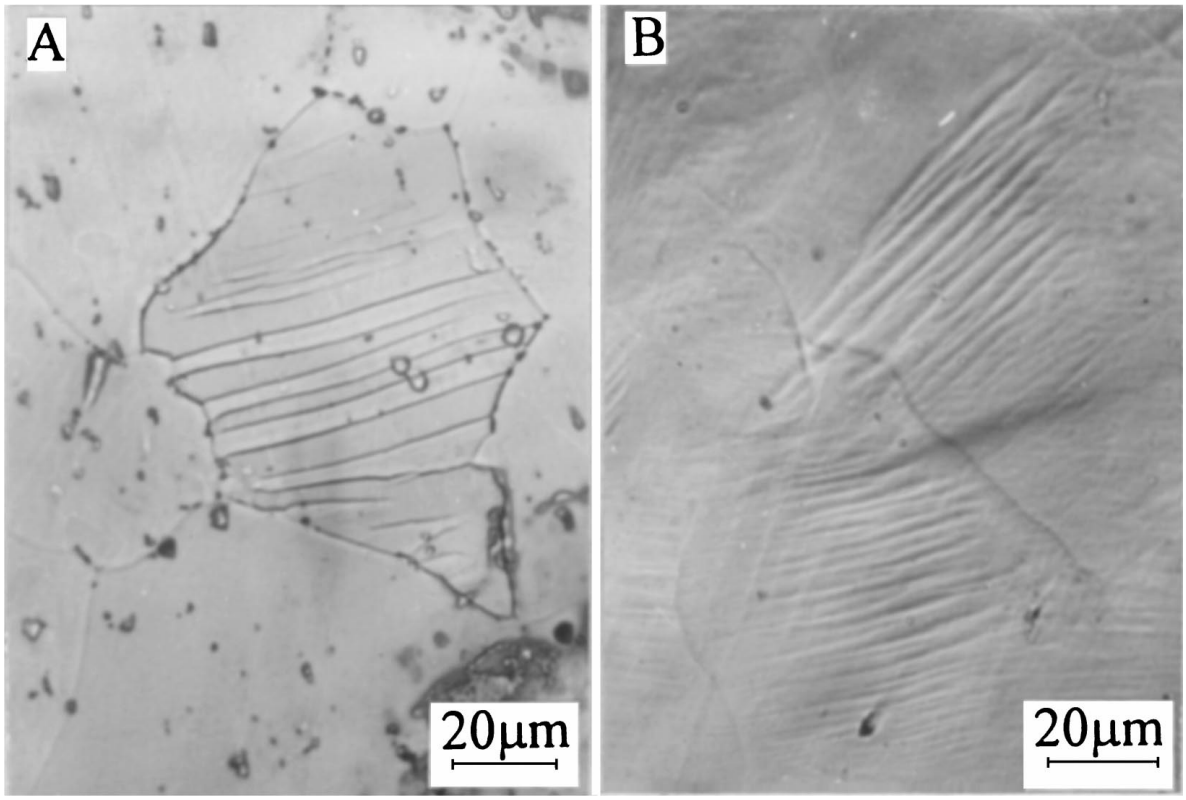

Figure 5 Slip lines produced in tension at room temperature showing (a) coarse, straight slip in Fe-28Al alloy and (b) wavy and finer slip in Fe-28Al-1.5Mn alloy.

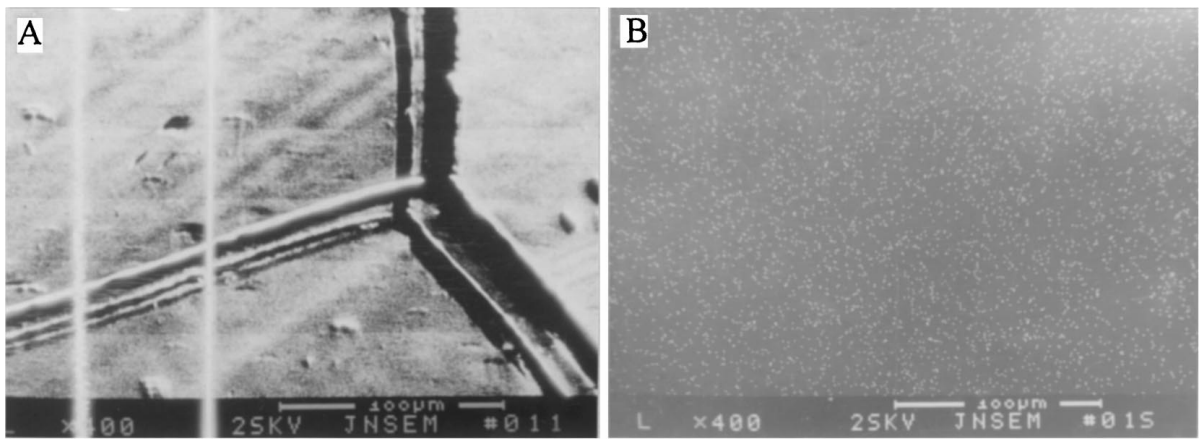

Figure 6 Electron probe micrographs of manganese in Fe-28Al-1.5Mn using (a) line scanning and (b) face scanning.

low ordering energy after Mn addition. The smaller the electronegative difference between two kinds of atoms, the bigger the interactive force between them and then the lower their ordering energy. Low ordering energy could propagate more formation of the ordering domain. Fine APD size makes more APDs exist and then reduces long-range order degree in the alloy.

The APB energy increases with the interaction potential between atoms and then with the ordering energy associated with atomic bonds. Substitution of some pairs of Mn-Al atoms for some pairs of Fe-Al atoms could reduce ordering energy and then reduce E_{APB}, propagating decomposition of superdislocations. The observed increase of dislocation space in the alloy with Mn addition could allow more uncoupling of the dislocations and more cross slip processes to occur, while still retaining some of the lattice friction and pinning mechanisms associated with coupled superdislocations. The additional cross slip results in the wavy slip lines (Fig. 5b) and zigzag APBs (Fig. 4d). The separation of dislocation spacing can be an indication of the relative strength of the APB energy which can be calculated by equating the repulsive force F_R and the APB energy E_{APB} for the plane to be considered [16]:

$$E_{APB} = F_R = \frac{Gb^2}{2\pi R}\left[\sin^2\theta + \frac{\cos^2\theta}{1-\nu}\right] \qquad (2)$$

where G is the shear modulus, **b** is the Burgers vector, R is the separation between dislocations, ν is Poisson's ratio, and θ is the angle between the dislocation line

and the Burgers vector. This equation indicates that as the dislocation spacing increases, the APB energy decreases.

The perfect DO_3 superdislocations are of twofold and fourfold. The twofold superdislocations are connected only by $\frac{a'}{2}\langle 1\,0\,0\rangle$ NNNAPB which slip more easily, similarly to B_2 superdislocations while fourfold superdislocations are connected by $\frac{a'}{4}\langle 1\,1\,1\rangle$ NNAPB and $\frac{a'}{2}\langle 1\,0\,0\rangle$ NNNAPB which make DO_3 Fe_3Al deform with difficulty (where a' is DO_3 superlattice constant). As E_{NNNAPB} is usually much lower than E_{NNAPB} in DO_3 Fe_3Al, and Mn addition retards formation of fourfold superdislocations, it could be suggested that twofold superdislocations in the alloy with Mn are B_2-type which have lower E_{NNNAPB} and are easier to slip. The deformation process in the DO_3 Fe-28Al-1.5Mn alloy, from Fig. 3 and Fig. 4, can been described as follows: twofold superdislocations slip at the beginning of deformation, the twofold superdislocations slip and decompose gradually into unit dislocations and the unit dislocations slip and slip cross as deformation increases. The mechanism of deformation is controlled at first by twofold superdislocation and at last by unit dislocation.

5. Conclusions

1. The addition of 1.5% manganese into DO_3 Fe-28Al alloy can decrease ordering degree and APD size in the alloy.

2. The slip systems are $\{1\,1\,0\}\ \langle 1\,1\,1\rangle$ in the DO_3 Fe_3Al with Mn addition. Mn could not change the slip systems in DO_3 Fe_3Al alloy.

3. Mn retards formation of fourfold superdislocation. In DO_3 Fe-28Al-1.5Mn alloy, the superdislocations are mainly twofold type. As the alloy deforms, the twofold superdislocation gradually decomposes into unit dislocation. The benefit of Mn addition to the ductility of Fe-28Al is thus believed to be a combined effect of easier slip and cross slip of twofold superdislocations and unit dislocations.

Acknowledgements

The authors would like to thank Professor Lu Guanglie for X-ray diffraction measurements.

References

1. R. C. CARWFORD, I. L. F. RAY and D. J. H. COCKAYNE, *Phil. Mag.*, **27** (1978) 1.
2. H. J. LEAMY, F. X. KAYER and M. J. MARCINKOWSHI, *Phil. Mag.*, **20**, (1969) 779.
3. Y. HUANG, Z. SHUN, W. YANG and G. CHENG, *Chinese Transactions of Non-Ferrous Material*, **4** (supplement) (1994) 131.
4. C. G. McKAMEY, J.A. TORTON and C.T. LIU, *J. Mater. Res.* (4), (1989) 1156 .
5. D. G. MORRIS, M. M. DADRAS and M. A. MORRIS, *Acta Metall. Mater.* **41**, (1993) 97.
6. K. YOSHIMI, H. TERASHIMA and S. HAMAKA, *Mater. Sci. Eng.* **194A**, (1995) 53.
7. W. YAN, Y. YANG and J. LIU, The First Pacific Rim International Conference on Advanced Materials and Processing (PRICM-1), Edited by C. SHI, H. LI and A. SCOTT (MMMS), 1992:785.
8. D. LI, D. LIN, A. SHAN and Y. LIU, *Scrip. Metall.* **30** (1994) 655.
9. B. LOU, M. LIU, J. TU, Z. MAO, Y. XIAO and Y. ZHONG, *Functional Mater.* **26** (supplement), (1996) 545.
10. B. LOU, M. LIU, J. TU, Z. MAO, Y. XIAO and Y. ZHONG, *Transactions of Metal Heat Treatment*, **17**(1), (1996) 58.
11. M. J. MARCINKOWSHI and N. BROWN, *J. Appl. Phy.*, **33** (2), (1961) 537.
12. H. LU, C. MA, K. LANG and L. MA, *Transactions of Metal Heat Treatment* **14** (1993) 50.
13. G. ATHANASSIADIS, A. Le CAER, J. FOCT and L. KIMLINGER, *Phys. Stat. Sol.* **40** (1977) 425.
14. M. G. MENDIRATTA and S. K. EHLERS, *Metall. Trans. A*, **14A** (1983) 2435.
15. A. O. MEKHRABOV, A. RESSAMOGLU and T.ÖZTÜRK, *J. Alloys. Comp.* **205** (1994) 147.
16. N. S. STOLOFF and R. G. DAVIES, In Progresin Material Science, edited by Bruce Chalmers and W. Hume-Rotherry (Pergamon Press, Oxford, 1966) Vol. 13, p. 1–84.

Received 1 November 1997
and accepted 16 July 1998